

Adrenocortical carcinoma survival rates correlated to genomic copy number variants

Elizabeth A. Stephan,¹ Tae-Hoon Chung,²
Clive S. Grant,⁴ Seungchan Kim,^{2,5}
Daniel D. Von Hoff,³ Jeffrey M. Trent,¹
and Michael J. Demeure^{3,6}

¹Genetic Basis of Human Disease Division, ²Computational Biology Division, and ³Clinical Translational Research Division, Translational Genomics Research Institute, Phoenix, Arizona; ⁴Department of Surgery, Mayo Clinic, Rochester, Minnesota; ⁵School of Computing and Informatics, Ira Fulton School of Engineering, Arizona State University, Tempe, Arizona; and ⁶Department of Surgery, University of Arizona, Tucson, Arizona

Abstract

Adrenocortical carcinoma (ACC) is a rare endocrine malignancy accounting for between 0.02% and 0.2% of all cancer deaths. Surgical removal offers the only current potential for cure. Unfortunately, ACC has undergone metastatic spread in 40% to 70% of patients at the time of diagnosis. Standard chemotherapy with mitotane is often ineffective with intolerable side effects. The modern molecular technology of comparative genomic hybridization allows the examination of DNA for chromosomal alterations, which can lend biological insight into cancer processes. Genomes of 25 ACC clinical samples were queried on the Agilent 44K Human Genome comparative genomic hybridization array detecting regions of chromosomal gain and loss within the tumor population. Commonly shared amplifications appearing in $\geq 50\%$ of tumors at $P \leq 10^{-4}$ include regions within chromosomes 5, 7, 12, 16q, and 20. Deleted genomic regions within ACC include portions of chromosomes 1, 3p, 10q, 11, 14q, 15q, 17, and 22q. Genomic aberrations in regions associated with differential survival ($P \leq 0.05$) and presence in $\geq 20\%$ of tumors include amplifications of 6q, 7q, 12q, and 19p. Deletions within stratified survival groups include localized regions within 3, 8, 10p, 16q, 17q, and 19q. Statistical

analysis of this genetic landscape reveals a set of chromosomal aberrations strongly associated with survival in an accumulation-dependent fashion. These regions may hold prognostic indicators and offer therapeutic targets that can be used to develop novel treatments for aggressive tumors. [Mol Cancer Ther 2008;7(2):425–31]

Introduction

Adrenocortical carcinoma (ACC) is one of the least commonly occurring but deadliest cancers. With an incidence of less than 0.77 in 1 million people, fewer than 250 new cases of ACC are seen within the United States each year (1). Carcinoma of the adrenal cortex accounts for between 0.02% and 0.2% of all cancer deaths (2, 3). The prognosis is poor with a 5-year survival rate of 20% to 45% due to typically late presentation and the limited effectiveness of broad-spectrum chemotherapy (4, 5). The standard chemotherapeutic treatment for this disease, since 1960, remains mitotane (Bristol-Myers Squibb), a derivative of the pesticide DDT (6). Response rates are poor ($\sim 22\%$), although survival for those who do respond is improved from 14 to 50 months (7). Due to the lack of effective treatments for ACC, increased knowledge of the cellular processes involved in oncogenesis is necessary for the development and implementation of targeted therapies.

Some have argued that the development and growth of ACC tumors is a multistep progression with accumulation of genetic alterations (8). Although ACC does occur in the context of inherited syndromes, such as the Li-Fraumeni and Beckwith-Wiedemann syndromes, most cases are of a sporadic nature. The Li-Fraumeni syndrome is traced to a germ-line mutation in the p53 tumor suppressor gene on chromosome 17p13 (9, 10). The genetic basis for the Beckwith-Wiedemann syndrome is an allelic loss at chromosome 11p15 (11). Characteristic mutations of both syndromes have been observed in some sporadic adrenocortical cancers (12, 13).

Knowledge of genomic gains, losses, and translocations associated with sporadic adrenocortical cancer has not yet revealed an ACC oncogenic pathway. Studies of the chromosomal and molecular abnormalities in ACC have relied on technologies, such as conventional comparative genomic hybridization (CGH) or fluorescence *in situ* hybridization, to identify genomic gains and losses.

Recent advances in modern array-based molecular genetic technologies offer the opportunity to study tumors with greater resolution and in a high-throughput fashion with the end goals of understanding oncogenesis, enabling the development of diagnostics and targeted therapies. Zhao et al. suggested that gains in DNA copy number in chromosome 17 or 17q represent the earliest genomic changes and are seen in benign adrenocortical adenomas

Received 4/11/07; revised 10/9/07; accepted 12/31/07.

Grant support: Advancing Treatments for Adrenocortical Carcinoma Fund.

The costs of publication of this article were defrayed in part by the payment of page charges. This article must therefore be hereby marked *advertisement* in accordance with 18 U.S.C. Section 1734 solely to indicate this fact.

Note: Array CGH data have been deposited in Gene Expression Omnibus (accession no. GSE7482).

E.A. Stephan and T-H. Chung contributed equally to this work.

Requests for reprints: Elizabeth A. Stephan, Genetic Basis of Human Disease Division, Translational Genomics Research Institute, 445 North 5th Street, Phoenix, AZ 85004. Phone: 602-343-8817; Fax: 602-343-8840. E-mail: estephan@tgen.org

Copyright © 2008 American Association for Cancer Research.

doi:10.1158/1535-7163.MCT-07-0267

only (14). Additional studies have identified loss of heterozygosity at 17p13 and 11p15 along with increased expression of insulin-like growth factor 2 as molecular events associated with progression toward a malignant phenotype (15). As reported by Dohna et al., gains and high-level amplifications in chromosomes 7, 14, and 19 were seen only in ACC and not in benign adrenocortical neoplasms, suggesting that these events may be late genetic perturbations in tumorigenesis (16). Deletions have also been found within chromosomes 1p and 17p implicating potential losses of tumor suppressor genes in these regions, marking the progression of benign adrenal adenoma to ACC (17). Similar to other cancers, there is evidence that the number of genetic aberrations increases as a factor of tumor growth and this size progression has been correlated with malignancy (14, 18, 19).

Herein, we use high-density CGH array analysis to identify genomic aberrations associated with poor survival as potential prognostic markers and therapeutic targets in aggressive ACC.

Materials and Methods

Clinical Samples

The total set of 25 ACC tumors includes 21 flash-frozen tumor samples collected between 1987 and 2003 at the Mayo Clinic. The subsequent 4 ACC tumors were acquired through collaborations with the University Hospital Essen and the University of Calgary. Research consent was obtained at the respective institutes through accepted institutional review board protocols and accepted into our research program and tumor bank under the Western Institutional Review Board–approved protocol no. 20051769. Extensive clinical and demographic information was collected at time of diagnosis and surgery (Supplementary Data 1).⁷

Comparative Genomic Hybridization

DNA extraction from flash-frozen ACC tumor samples was done following the standard protocol for the Qiagen DNeasy Blood and Tissue Kit (Qiagen). Oligo-based CGH was done according to manufacturer's instructions for the Agilent Human Genome Microarray Kit 44B (Agilent Technologies) starting with 800 ng DNA from clinical samples and a separate reference sample of 800 ng control male genomic DNA (Promega). Experimental samples labeled with Cy5 and reference samples labeled with Cy3 (GE Healthcare) were combined and hybridized to a single CGH array. Deviating from the Agilent Oligo aCGH Hybridization Kit protocol, samples were incubated with Cot1 (1 mg/mL), 10× blocking solution, and 2× hybridization buffer at 99°C for 3 min, 37°C for 30 min, and centrifuged at high speed for 1 min. The samples were hybridized according to Agilent protocol. Arrays were washed, scanned, and data extracted using Agilent Feature Extraction 8.1. Data for arrays fulfilling standard Agilent

quality requirements were included in further statistical analyses.

Statistical and Survival Analyses

The log₂ of Cy5 and Cy3 ratio (log-ratio) was used as the measure of copy number ratio between tumor and normal samples throughout the analysis. To detect the regions of copy number aberration, log-ratio values of a sliding window of 25 probes in length were compared using the Wilcoxon's rank-sum test with the log-ratio values of an artificial reference chromosome constructed for each tumor (20). The reference chromosome was created by recursively accepting 25 randomly sampled log-ratio values from the autosomal regions with *P* value of Wilcoxon's signed rank test (against 0) > 0.05 until the size reached 1,000. The *P* values and corresponding false discovery rates (or *q* values) for the copy number gain or loss (indicated as *P*_{gain} and *Q*_{gain} or *P*_{loss} and *Q*_{loss}) were calculated independently for each sliding window and assigned to the center position of the window.

Commonly shared genomic aberrations in ACC tumors were identified by gathering overlapping sliding windows that were gained or lost by ≥50% of all ACC patients. A sliding window was called gained if *P*_{gain} < 10⁻⁵ and *Q*_{gain} < 10⁻⁴ and lost if *P*_{loss} < 10⁻⁵ and *Q*_{loss} < 10⁻⁴. The statistical significance of an identified region was evaluated by testing the distribution of copy number changed tumor fractions of sliding windows contained in the region against the ratio cutoff 0.5 using Wilcoxon's signed rank test.

The clinical implication of the observed genomic aberrations was examined in detail by identifying chromosomal regions whose gains or losses were associated with the overall survival difference using the log-rank test for all sliding windows across the genome. Sliding windows whose gains or losses were linked to poor prognosis (*P* ≤ 0.05) and occurred in ≥20% of all patients were called survival relevant and retained for further analysis.

Unsupervised clustering of a summary matrix was done to detect the coappearance of survival relevant genomic aberrations from different chromosomal regions. For each chromosome that contained survival relevant sliding windows, the survival relevant region was identified first by collecting all survival relevant sliding windows across all patients within it. Then a summary indicator was scored for the chromosome of a patient as +1 (gain), 0 (no change), or -1 (loss) if >50% of sliding windows that fell within the survival relevant region of the patient harbored corresponding genomic aberrations. In the clustering, the distance between two vectors was measured by counting the number of elements that were not the same and the complete linkage was used to determine the distance between two intermediate clusters.

Results

Common Genomic Aberrations

Genomic aberrations are visualized as the histogram of copy number change frequencies over all ACC tumors

⁷ Supplementary material for this article is available at Molecular Cancer Therapeutics Online (<http://mct.aacrjournals.org/>).

(Fig. 1A) and the heat map of chromosomal gain and loss for individual patients (Fig. 1B). The copy number aberration frequency plot (Fig. 1A) represents the fraction of patients with $P \leq 10^{-5}$ and $q \leq 10^{-4}$ for each sliding window. The results clearly indicate that ACC tumors have an extensive level of genomic aberrations as has been reported previously (Table 1). In most of the chromosomes, common aberrations (gains or losses) encompassing large fractions of the samples are observed, indicating high occurrence of genomic change. The most distinctive aberrant regions include gains of chromosomes 5, 6q, 7, 8q, 12, 16q, and 20 and losses of chromosomes 1, 2q, 3, 6p, 7p, 8p, 9, 10, 11, 13q, 14q, 15q, 16, 17, 19q, and 22q (visualized in Fig. 1 and detailed in Supplementary Data 2).

Survival Relevant Genomic Aberrations

Chromosomal regions were further analyzed to determine if the occurrence of genomic aberrations was associated with survival difference. Figure 2 shows the distribution of log-rank test P values across the genome. The P values above and below the X axis represent the association between gains and losses (respectively) and survival difference. Specific genomic aberrations associated with worse survival rates are detailed in Table 2 with gains in 6q, 7q, 12q, and 19p and losses in 3, 8, 10p, 16q, 17q, and 19q. Survival curves created for each aberration linked to poor survival can be seen in Supplementary Data 3.

To clarify possible coappearances of survival relevant genomic aberrations, unsupervised hierarchical clustering was done with sliding windows in regions relevant to

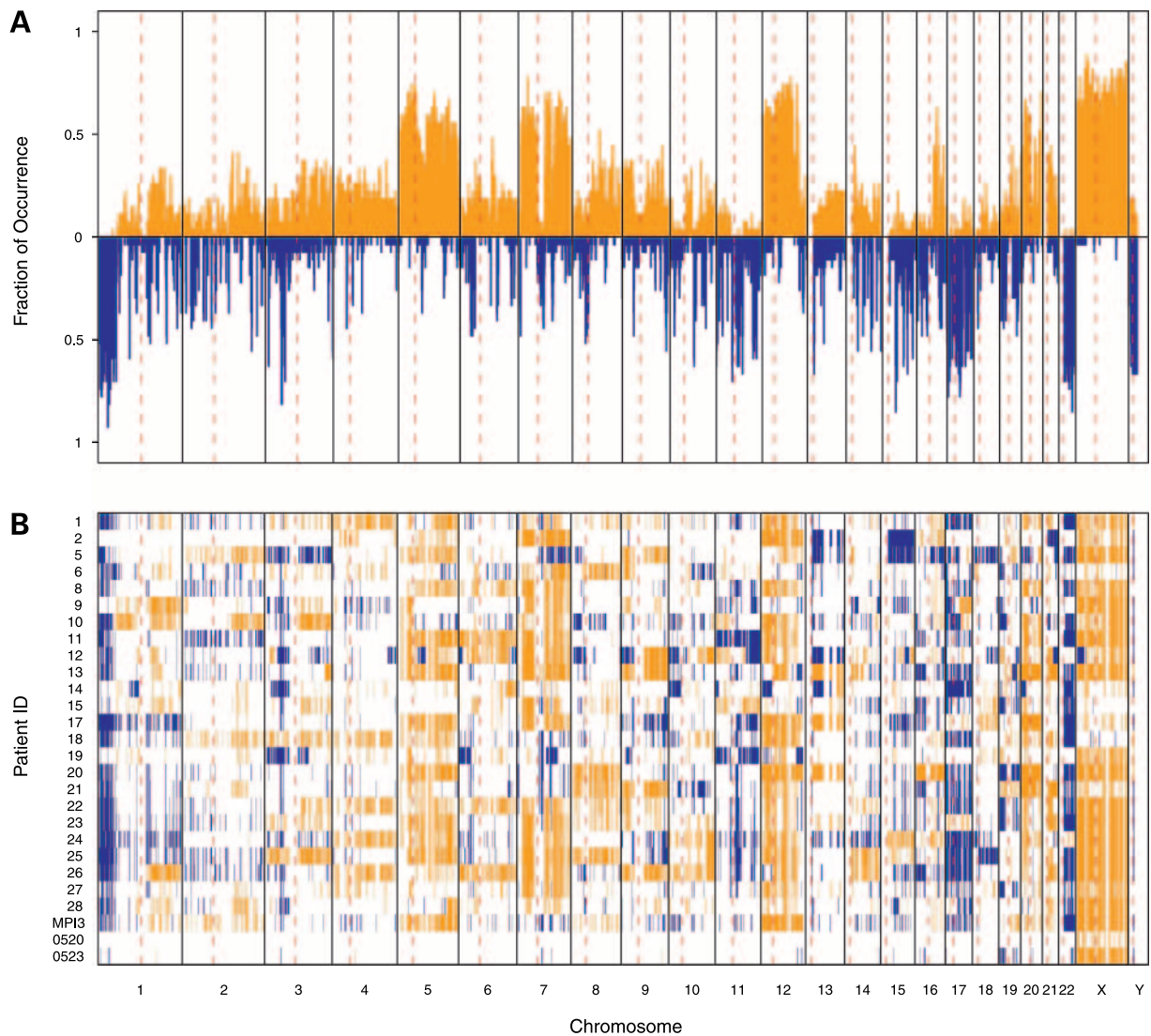


Figure 1. Genomic aberrations in ACC samples. Relative gain and loss across the genomes of 25 ACC samples calculated as sliding window segments of 25 probes. **A**, gains (orange) and losses (blue) across chromosomes as a measure of rate of occurrence with $P \leq 10^{-5}$ and $q \leq 10^{-4}$. **B**, individual patient aberration profiles at a 1-Mb resolution across chromosomes.

Table 1. Summary of previous genomic analyses in ACC

No. ACCs	Genetic analysis	Regions gained	Regions lost	Reference
12	Conventional	CGH 5q12-q13, 5q22-qter, 9q32-qter, 12q13-q14, 12q24, 20q, Xq13-q21	1p21-p31, 1q23-q41, 2p21-pter, 2q, 3p, 3q, 6q, 9p, 11q14-qter, 18q	(14)
14	Conventional CGH	1p34.3-pter, 1q22-q25, 3p24-pter, 3q29, 5, 7, 7p11.2-p14, 8, 9q, 9q34, 11q, 11q12-q13, 12q, 12q13, 12q24.3, 13q34, 14q, 14q11.2-q12, 14q32, 16, 16p, 17q, 17q24-q25, 19, 19p13.3, 19q13.4, 20, 22q, 22q11.2-q12	9p	(16)
13	Conventional CGH	4, 5, 12, 12q14-q21, 19	1p, 1p34-pter, 2q, 2q34-qter, 11q, 11q24-qter, 17p, 17p13-pter, 22	(17)
8	Conventional CGH	4q, 4q31, 5, 12, 12cent-q24, 15q, 15q21-qter, 16q, 19p	2, 2p23-cent-q21, 3p21-cent, 6q, 8p, 9p, 11p, 11q, 11q22-qter, 17p, 17q, 18q, 22q	(18)
12	Conventional CGH and oncogene-specific microarray	1q, 4p15-pter, 5p, 5p15, 5q, 5q13, 5q32-qter, 7p, 7q, 8q, 8q24, 9p, 9q, 12q13-q15, 13q, 16q, 17p, 17q, 20p, 20q		(19)

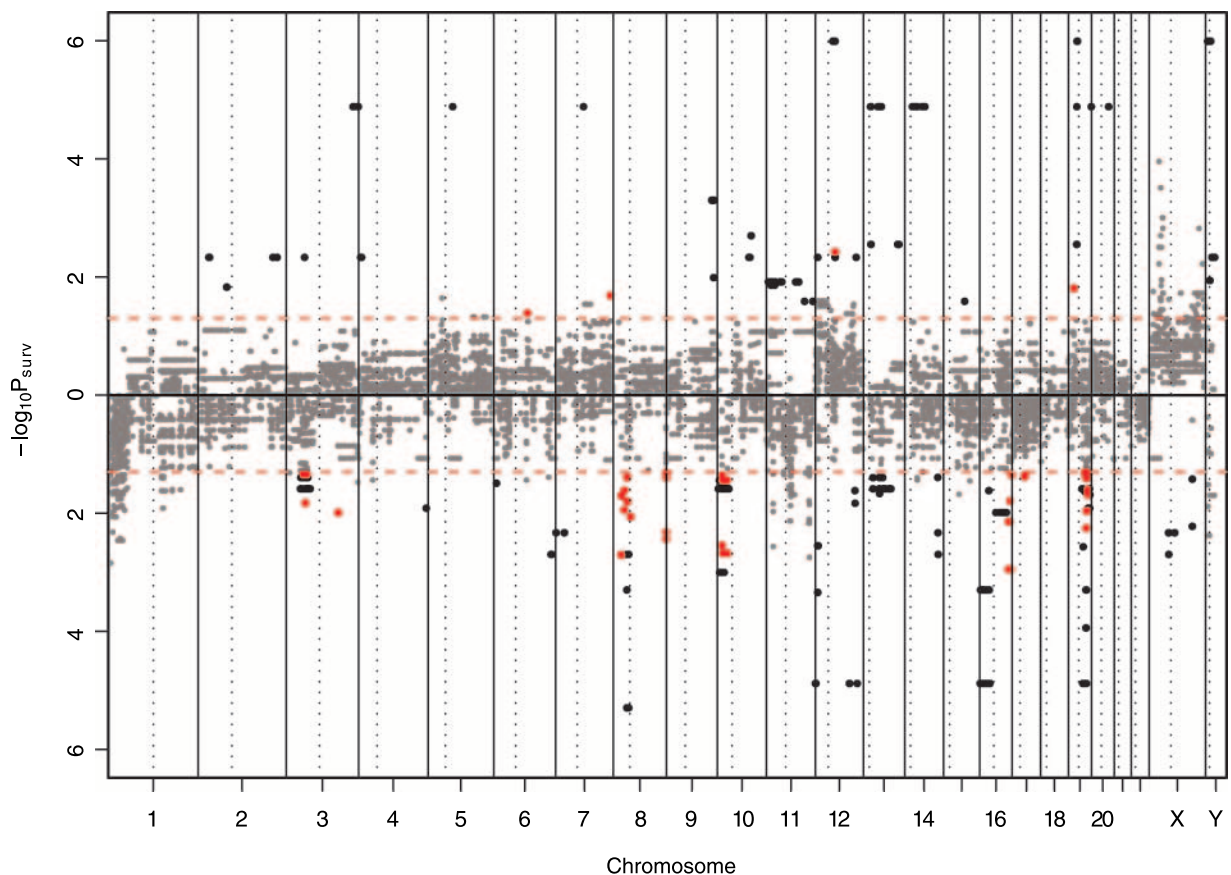


Figure 2. Genomic aberrations linked to survival. Gains and losses across the ACC genome are plotted as the $-\log_{10} P$ value of survival analysis. *Black*, segments with genomic aberration preferentially found in patients with significantly shorter survival after surgery with $P \leq 0.05$; *red*, segments present in $\geq 20\%$ of all ACC samples.

Table 2. Aberrations with high representation in poor survival

	Chromosome	Cytogenic band	Segment start	Segment end	Segment length
Gain	6	6q15-6q16.1	91152410	95641352	4488942
	7	7q36.1	150275058	151470304	1195246
	12	12q13.2	54496959	54887816	390857
	19	19p13.12-19p13.11	15352798	16118051	765253
Loss	3	3p21.31	46534671	47516603	981932
	3	3p21.31	49687490	50219610	532120
	3	3p21.1	52432656	53876467	1443811
	3	3q23	142987765	144031265	1043500
	8	8p21.3	21408650	22539377	1130727
	8	8p21.1-8p12	29147511	31607545	2460034
	8	8p12-8p11.23	36481039	39128088	2647049
	8	8q24.3	144753570	146201712	1448142
	10	10p14-10p13	11285212	16864223	5579011
	10	10p12.1	26030462	27568983	1538521
	16	16q23.2-16q23.3	79195214	80590034	1394820
	16	16q24.1	82774218	84680399	1906181
	16	16q24.1-16q24.2	85171711	86599633	1427922
	16	16q24.3	87455812	88254372	798560
	17	17q12	33805634	34663603	857969
	19	19q13.2	45108448	45718366	609918
19	19q13.31-19q13.32	49537470	50323207	785737	
19	19q13.32	50358143	53057498	2699355	
19	19q13.32-19q13.33	53210832	53917176	706344	

NOTE: Segment lengths are measured in kilobases according to the National Center for Biotechnology Information Build 36 of Human Genome Map.

survival difference (see Materials and Methods for details). The results shown in Fig. 3A indicate that genomic aberrations relevant to survival difference in unique chromosomes do not cosegregate. Furthermore, the clustering of samples results in three sample groups, each of which is associated with varying presence of selected aberrations. The groups are differentially associated with survival trends given by a Kaplan-Meier analysis *P* value of 7.4×10^{-6} (Fig. 3B). Additional tumor characteristics (Fig. 3A) are not associated with the described survival difference, indicating that the survival clusters are dependent on accumulation of genomic aberrations alone.

Discussion

With few therapeutic options and a poor understanding of ACC oncogenesis, emerging high-density genomic scanning technologies enable identification of genomic events linked to disease. Table 1 summarizes previous genomic analyses of ACC tumors presented in five publications. A new, more precise high-resolution technology is used in the present study to identify genomic aberrations in ACC with >44,000 60-mer oligonucleotide probes spaced across the entire genome. Compared to the conventional CGH or interphase fluorescence *in situ* hybridization, which offer a resolution of ≤ 10 Mb, new Agilent chip-based array CGH offers a much improved resolution with probes on average every 35 kb (21). The previous studies of chromosomal amplifications and deletions used sample sets between

8 and 14 adrenocortical tumors. In the present study, we used high-resolution CGH to analyze 25 ACC samples for genetic gains and losses within the tumor population.

Array-based CGH analysis identifying chromosomal aberrations shared among a high percentage of ACC tumors gives a superior evaluation of areas characteristically linked to ACC oncogenesis. Genomic aberrations within the ACC genome (Fig. 1A) illustrate the overall gains within chromosomes 5, 6q, 7, 8q, 12, 16q, and 20 and losses within chromosome 1, 2q, 3, 6p, 7p, 8p, 9, 10, 11, 13q, 14q, 15q, 16, 17, 19q, and 22q (Supplementary Data 2). These high-resolution results recapitulate genomic abnormalities presented in past research (see Table 1). Of note, the analysis identified unique losses in 10q, 14q, and 15q, giving a more comprehensive characterization of the ACC genomic landscape. Genes within these regions can give insight into the pathways of oncogenesis active within ACC. Among other deleted regions, literature suggests that the loss of chromosomes 1p and 17p are linked to progression from benign to malignant ACC (17). Recent studies have identified a chromodomain helicase DNA-binding protein 5 within 1p36.31 as a tumor suppressor gene (22, 23). The absence of this protein allows uncontrolled cell growth and immortalization through the p19^{Arf}/p53 pathway (22). With mutations of p53 observed in Li-Fraumeni syndrome (with associated development of ACC), the loss of chromodomain helicase DNA-binding protein 5 may act as an additional hit within this pathway, increasing malignant growth, proliferation, and a lack of

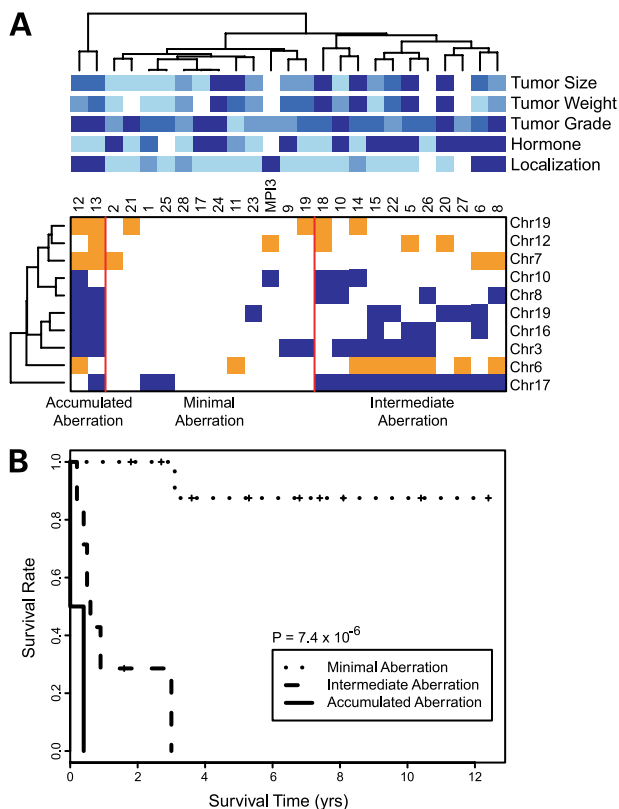


Figure 3. Aberration abundance associated with survival. **A**, hierarchical clustering of chromosomal aberrations linked to survival (from Fig. 2). Orange, genomic gains; blue, genomic losses. Samples cluster into three groups representing minimal, intermediate, and accumulated levels of CGH aberrations. Tumor characteristics across accumulation clusters (from **A**) are then mapped onto the clustering matrix. Tumor size, tumor weight, and tumor grade are colored from level 1 (light blue) to level 4 (dark blue). Tumor size was categorized as ≤ 8 cm (level 1), 8 to 9.5 cm (level 2), 9.5 to 15 cm (level 3), and > 15 cm (level 4), and tumor weight was grouped as ≤ 139.5 g (level 1), 139.5 to 195 g (level 2), 195 to 887.5 g (level 3), and > 887.5 g (level 4). Hormonal activity is colored from light blue to dark blue in the order of cushings, aldosterone, feminizing, and nonfunctional states. The degree of tumor localization is colored from light blue to dark blue in the order of localized, regional, and metastatic states. White boxes, information. **B**, survival analysis of abundance clusters identifies associated survival differences at a Kaplan-Meier P value between the three groups of 7.4×10^{-6} .

apoptosis. It is the elucidation and validation of these proposed pathways that will lead to an understanding of ACC oncogenesis.

Linking genomic events to clinical phenotype further increases the characterization of cancerous processes. Analysis of Kaplan-Meier survival curves for common aberrations identified a set of genomic gains and losses occurring specifically within populations with shortened survival rates. As illustrated in Fig. 2, genomic aberrations in red show selective presence in $\geq 20\%$ of patients with short postsurgical survival. The regions include gain of 6q, 7q, 12q, and 19p and loss of 3, 8, 10p, 16q, 17q, and 19q (Table 2). These regions further cluster by accumulation of aberrations (Fig. 3A) and survival analysis identified an

association between level of accumulation and survival rate (Fig. 3B). It is hypothesized that an increase in total aberrations, and not a combination of specific aberrations, links to shortened survival. This situation would indicate increasing genomic aberration with progressing disease. Multistep cancer progression cannot be illustrated in this data set due to the absence of analysis on benign adrenal tumors. Addition of benign and early-stage ACCs will allow development of a cancer progression model.

Disease variables, such as tumor size, tumor weight, tumor grade, functionality, and localization, were not shown to be significantly linked to the described survival differences (Fig. 3A). It is not clear whether these clinical variables truly have no effect on survival or whether there is insufficient statistical power (due to small sample size) to identify the underlying clinical stratifications.

Herein, high-resolution CGH has been used to characterize genomic differences between a group of 25 ACC tumors and normal DNA. These areas of gain and loss give insight into the mechanisms of disease and identify genomic regions containing potential targets for therapeutic intervention. Accumulation of gains and losses in specific regions can also be linked with survival difference, creating a genetic footprint for ACC survival and progression of disease.

References

- Kebebew E, Reiff E, Duh QY, Clark OH, McMillan A. Extent of disease at presentation and outcome for adrenocortical carcinoma: have we made progress? *World J Surg* 2006;30:872–8.
- Wajchenberg BL, Albergaria Pereira MA, Medonca BB, et al. Adrenocortical carcinoma: clinical and laboratory observations. *Cancer* 2000;88:711–36.
- Crucitti F, Bellantone R, Ferrante A, Boscherini M, Crucitti P. The Italian Registry for Adrenal Cortical Carcinoma: analysis of a multiinstitutional series of 129 patients: the ACC Italian Registry Study Group. *Surgery* 1996;119:161–70.
- Icard P, Goudet P, Charpenay C, et al. Adrenocortical carcinomas: surgical trends and results of a 253-patient series from the French Association of Endocrine Surgeons study group. *World J Surg* 2001;25:891–7.
- Demeure MJ, Somberg LB. Functioning and nonfunctioning adrenocortical carcinoma: clinical presentation and therapeutic strategies. *Surg Oncol Clin N Am* 1998;7:791–805.
- Bergental DM, Hertz R, Lipsett MB. Chemotherapy of advanced adrenocortical cancer with o'p'DDD. *Ann Intern Med* 1960;53:672–82.
- Decker RA, Elson P, Hogan TF, et al. Eastern Cooperative Oncology Group study 1879: mitotane and Adriamycin in patients with advanced adrenocortical carcinoma. *Surgery* 1991;110:1006–13.
- Sidhu S, Sywak M, Robinson B, Delbridge L. Adrenocortical cancer: recent clinical and molecular advances. *Curr Opin Oncol* 2003;16:13–8.
- Srivastava S, Zou ZQ, Pirolo K, Blattner W, Chang EH. Germ-line transmission of a mutated p53 gene in a cancer-prone family with Li-Fraumeni syndrome. *Nature* 1990;348:747–9.
- Malkin D, Li FP, Strong LC, et al. Germ line p53 mutations in a familial syndrome of breast cancer, sarcomas, and other neoplasms. *Science* 1990;250:1233–8.
- Henry Ik, Bonaiti PC, Chehense V, et al. Uniparental paternal disomy in a genetic cancer-predisposing syndrome. *Nature* 1991;351:665–7.
- Ohgaki H, Kleihues P, Heitz PU. p53 mutations in sporadic adrenocortical tumors. *Int J Cancer* 1993;54:408–10.
- Gicquel C, Raffin Sanson ML, Gaston V, et al. Structural and functional abnormalities at 11p15 are associated with the malignant phenotype in sporadic adrenocortical tumors: study on a series of 82 tumors. *J Clin Endocrinol Metab* 1997;82:2559–65.

14. Zhao J, Speel EJM, Muletta-Feurer S, et al. Analysis of genomic alterations in sporadic adrenocortical lesions: gain of chromosome 17 is an early event in adrenocortical tumorigenesis. *Am J Pathol* 1999;155:1039–45.
15. Gicquel C, Bertagna X, Gaston V, et al. Molecular markers and long-term recurrences in a large cohort of patients with adrenocortical tumors. *Cancer Res* 2001;61:6762–7.
16. Dohna M, Reincke M, Mincheva A, Allolio B, Solinas-Toldo S, Lichter P. Adrenocortical carcinoma is characterized by a high frequency of chromosomal gains and high-level amplifications. *Genes Chromosomes Cancer* 2000;28:145–52.
17. Sidhu S, Marsh DJ, Theodosopoulos G, Philips J, Bambach CP, Campbell P. Comparative genomic hybridization analysis of adrenocortical tumors. *J Clin Endocrinol Metab* 2002;87:3467–74.
18. Kjellman M, Kallioniemi O-P, Karhu R, et al. Genetic aberrations in adrenocortical tumors detected using comparative genomic hybridization correlate with tumor size and malignancy. *Cancer Res* 1996;56:4219–23.
19. Zhao J, Roth J, Bode-Lesniewska B, Pfaltz M, Heitz PU, Komminoth P. Combined comparative genomic hybridization and genomic microarray for detection of gene amplifications in pulmonary artery intimal sarcomas and adrenocortical tumors. *Genes Chromosomes Cancer* 2002;34:48–57.
20. Chen QR, Bilke S, Wei JS, et al. cDNA array-CGH profiling identifies genomic alterations specific to stage and MYCN-amplification in neuroblastoma. *BMC Genomics* 2004;5:70.
21. Barrett MT, Scheffer A, Ben-Dor A, et al. Comparative genomic hybridization using oligonucleotide microarrays and total genomic DNA. *Proc Natl Acad Sci U S A* 2004;101:17764–70.
22. Bagchi A, Papazoglu C, Wu Y, et al. CHD5 is a tumor suppressor at human 1p36. *Cell* 2007;128:459–75.
23. Brodeur GM, Sekhon G, Goldstein MN. Chromosomal aberrations in human neuroblastomas. *Cancer* 1977;40:2256–63.